Hindawi
Geofluids
Volume 2022, Article ID 6755242, 12 pages
https://doi.org/10.1155/2022/6755242

Research Article

Experimental Investigation on the Pressure Distribution Law and Calculation Method of Muddy Water with High Silt Content

Lijia Zhong,[1] **Fengyin Liu**,[1] **Bo Wang**,[2] **Zhao Yang**,[1] **and Dong Zhou**[3]

[1]*Institute of Geotechnical Engineering, Xi'an University of Technology, China*
[2]*Jikan Research Institute of Engineering Investigation and Design, Co., Ltd., China*
[3]*Yellow River Engineering Consulting Co., Ltd., China*

Correspondence should be addressed to Lijia Zhong; 411459340@qq.com

Received 24 October 2021; Revised 30 November 2021; Accepted 11 December 2021; Published 4 January 2022

Academic Editor: Peng Hou

The pressure distribution law of muddy water with high silt content has great influence on the stress and strain calculation of the dam body. Currently, there is a few research studies referring to the calculation method of high silt content muddy water pressure, which leads to no reliable theoretical basis for muddy water pressure calculation in dam design. In this paper, muddy water with high silt content was prepared and the imitation tests and model tests were carried out to investigate the pressure distribution law. Based on the test result analysis, it is indicated that the muddy water with high silt content is also in a flowable and viscous state, which is consistent with the law of fluid behavior; the horizontal pressure is equal to the vertical pressure at the same position, and this relationship is generally time independent; through the test result analysis, a pressure formula for muddy water with high silt content is proposed; through comparison between the pressure formula-calculated results and monitoring data, it is indicated that the proposed pressure formula is applicable in the calculation of muddy water pressure. The formula can be a useful tool in the dam safety and design calculation.

1. Introduction

The water conservancy project is mainly constructed for preventing water disasters and reasonable use of water resources. And one of the functions of the dam is to intercept the flow, which creates conditions for the construction of geothermal resources in the water section. But high silt content in the river is a serious problem. According to the monitoring data before and after the construction of the power station, Yang et al. [1–3] summarized the basic situation of the silt problem of the Yellow River. The relevant data [4, 5] shows that the maximum silt content of the Yellow River in China was as high as 911 kg/m^3. High silt content has influence on the design, operation, and management of a hydropower station in different extents. The influence of muddy water on the dam body is mainly caused by lateral pressure. In particular in the dam design, the pressure distribution form of muddy water has great influence on the stress and strain calculation of the dam [6–9].

Xu [10] found that the lateral pressure coefficient is close to 1.0 when the water content of silt soil is approximately equal to its liquid limit. Chen and Cui [11, 12] calculated the stress of a gravity dam with the finite element method. The result showed that the silt sediment in front of the dam increased the lateral pressure of the dam body, and the influence of silt sediment should be taken into account when designing a gravity dam. Yang [13, 14] and Chen [15, 16] demonstrated that the height of the sediment on the upstream side of the dam was one of the main parameters for calculating silt load in the design of hydraulic structures. Han [17, 18] systematically studied the deposition process of silt. Yin et al. [19–21] conducted some experimental investigation on the silt on the upstream side dam. Chen [22–24] calculated the lateral active earth pressure by taking unit weight of silt as a constant value.

In addition, the distribution and transport of silt in rivers have been studied by Duc et al. [25, 26], Eriksson and Persson [27], Chalov et al. [28], Chang et al. [29, 30], and Gao

and Collins [31, 32]. He et al. [33] performed a simulation analysis of silt deposition with Delft3D. Campisano et al. [34] performed numerical simulation on the rectangular open channel bed volume using a uniform deposition semi-coupled method based on the 1D Saint–Venant–Ekner equation. Mateusz et al. [35], Angelika and Tamara [36], and Zuo et al. [37] estimated the accumulation rate of river deposits with the 210Pb method.

The overloads applied on the dam include self-weight, water pressure (hydrostatic pressure), silt pressure, etc. [38]. For the muddy water with low silt content, the silt particles are dispersed in muddy water, and the characteristics of the water are unchanged; correspondingly, the muddy water pressure can be calculated directly according to the formula of the hydrostatic pressure.

Formula (1) for pressure calculation of muddy water and formula (2) for horizontal silt pressure acting on the unit width of the dam surface are recommended in the *Design Specification for Concrete Arch Dams* [38].

$$p = \gamma_w \cdot H, \tag{1}$$

where p is the hydrostatic pressure (kPa) at the calculation depth, H is the water head (m) at the calculation depth, and γ_w is the unit weight of water (kN/m^3).

$$p_{sk} = \frac{1}{2}\gamma_{sb} h_s^2 tg^2\left(45^\circ - \frac{\varphi_s}{2}\right), \tag{2}$$

where p_{sk} is the horizontal pressure of silt (kPa), γ_{sb} is the buoyant unit weight of silt (kN/m^3), $\gamma_{sb} = \gamma_{sd} - (1 - n)\gamma_w$, γ_{sd} is the dry unit weight of silt, γ_w is the unit weight of water (kN/m^3), n is the porosity of silt, h_s is the silting thickness in front of the dam (m), and φ_s is the internal friction angle of the silt (°).

However, the flow characteristics of muddy water with high silt content are quite different from those of hydrostatic fluid. Considering the flow characteristic difference between muddy water and hydrostatic fluid, here the following are some basic problems: i.e., is the water pressure calculation method of formula (1) applicable? In formula (1), should γ_w take the unit weight of water or the unit weight of muddy water? What is the critical silt content between the two values? Those problems are not specified in detail currently.

Through above analysis, it is indicated that there are a few research works related to the pressure distribution law and pressure calculation formula for muddy water with high silt content and its influence on the dam stress. Therefore, it is necessary to carry out further relevant research. In this paper, a water conservancy project in the Yellow River in China is taken as a research object, with the prepared muddy water with high silt content, imitation and model tests are carried out, and the pressure distribution law is investigated.

2. Preparation of Muddy Water with High Silt Content

Based on the monitoring data of the water conservancy project in the Yellow River, the muddy water sample with the generally same sand gradation was prepared. And the measured annual average silt content of this hub project is 144 kg/m^3, and the maximum is 1428 kg/m^3.

Silt used in this paper is taken from undisturbed areas in the tidal flat of the Yellow River (Henan section). Add certain amount of silty clay to the silt and evenly stir it, and then, the particle analysis test was conducted. The particle size distribution curves are shown in Figure 1.

As shown in Figure 1, the particle composition of the prepared silt is close to the measured value of the actual silt. According to the silt content of the designed muddy water test, the prepared silt is mixed with the water of corresponding amount; then, fully stir evenly to prepare the muddy water required. The relationship between the silt-water mass ratio and silt content is shown in Formula (3)

$$\lambda = \frac{S}{1000 - S/G_s}, \tag{3}$$

where λ is the silt-water mass ratio, S is the silt content of muddy water, and G_s is the specific gravity of silt; take 2.65.

The relationship between silt content and unit weight and silt-water mass ratio of muddy water is shown in Table 1. The unit weight of muddy water-measured method is the U-tube method. The liquid and plastic limit of the test silt is 25.9% and 15.0%, respectively.

3. Details of the Pressure Imitation Test for Muddy Water with High Silt Content

3.1. Instruments for Test. The instrument used to the measurement of muddy water pressure is BGK4810 high-precision soil pressure gauge. The main structure is shown in Figure 2. When the soil pressure gauge is placed in muddy water, the water pressure will cause corresponding change in the fluid pressure in the pressure box. According to the reading of the vibrating wire pressure sensor and formula (4), the muddy water pressure is calculated as

$$P = G(R_1 - R_0) + K(T_1 - T_0), \tag{4}$$

where P is the pressure (kPa), G is the calibration coefficient (kPa/digit), K is the temperature coefficient (kPa/°C), R_0 and R_1 are the initial and current reading of the sensor (digit), respectively, and T_0 and T_1 are the initial and current temperature of the sensor (°C), respectively.

Figure 3 shows the installment of the pressure gauges in the pressure tank.

3.2. Steps of Imitation Tests. The imitation tests are conducted to simulate different water heads by using a manual pressure pump attached to the pressure tank to pressure the muddy water in it.

Then, measure the horizontal pressure P_1 of the muddy water in the closed pressure tank under a certain water head, and the corresponding vertical pressure P_2 is calculated to study the pressure distribution law of muddy water with high silt content under different water heads. The muddy

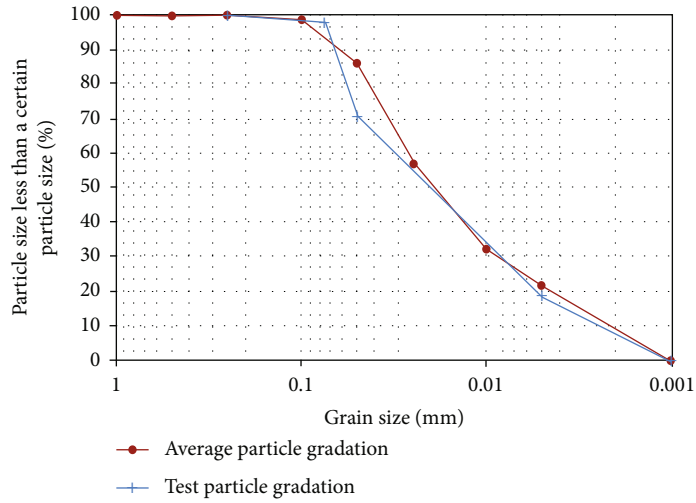

Figure 1: Particle gradation curves of artificially prepared silt and the measured data.

Table 1: Comparison of silt content and unit weight and silt-water mass ratio of muddy water.

Silt content S (kg/m^3)	Silt-water mass ratio	The unit weight of muddy water γ_w (kN/m^3)
100	1 : 9.62	10.41
200	1 : 4.62	11.02
300	1 : 2.96	11.63
400	1 : 2.12	12.24
500	1 : 1.62	12.85
600	1 : 1.29	13.46
700	1 : 1.05	14.07
800	1 : 0.87	14.68
900	1 : 0.73	15.29
1000	1 : 0.62	15.90

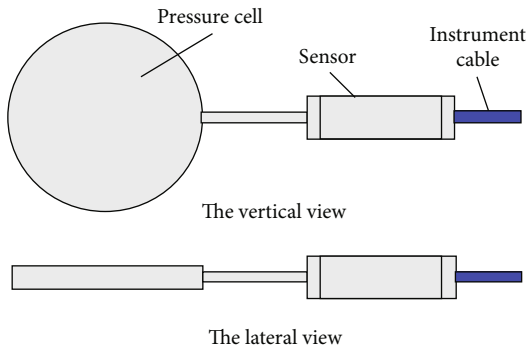

Figure 2: Structure diagram of soil pressure gauge.

water head at the midpoint of the soil pressure gauge in the pressure tank is approximately 0.515 m.

The imitation test steps are as follows:

(1) According to the needed silt content, the corresponding masses of silt and water are calculated by formula (3) and weighed. The water and the prepared silt are mixed to prepare the different required muddy water (our set silt content: 110.7 kg/m^3, 284.6 kg/m^3, 395.3 kg/m^3, 727.3 kg/m^3, and 1059.3 kg/m^3)

(2) Put the soil pressure gauge vertically into the pressure tank

(3) Inject the prepared high silt content muddy water into the pressure tank (see Figure 4)

(4) After sealing the pressure tank, a manual pressure pump was used to apply different water heads into the tank (see Figure 5). The pressure range is from 0 kPa to 400 kPa, and the pressure gradient is 50 kPa

(5) Read out the pressure gauge data, and calculate the horizontal pressure P_1 of each group of muddy water according to corresponding reading and formula (4).

(6) The properties of each group of muddy water are assumed to be consistent with the hypothesis of fluid characteristics. Referring to Table 1, the unit weight of each group of muddy water is calculated by the interpolation method. Then, the vertical pressure P_2, at the same position under each water head, is calculated, and P_2 is equal to the sum of the external pressure value and the pressure calculated according to the depth of the test point

(7) After the experiment, the muddy water was taken out and observed to determine whether the calculation assumption in step 6 is applicable

(8) If the assumption is appropriate, then the difference and ratio between horizontal pressure P_1 and vertical pressure P_2 of each group of muddy water are calculated, and the relationship curves with external pressure are drawn

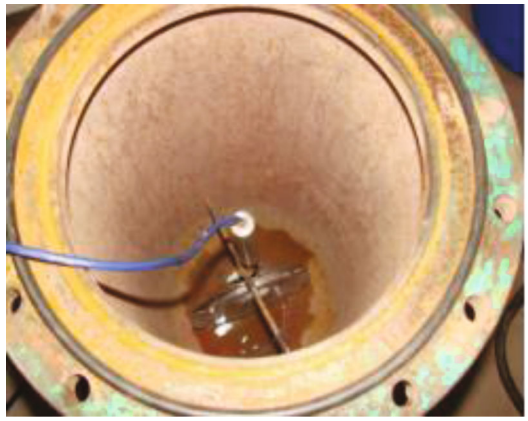

Figure 3: Installment of the pressure gauge in the pressure tank.

Figure 4: Muddy water is injected into the pressure tank.

Figure 5: Sealing the pressure tank and pressurizing it.

4. Details of the Pressure Model Test for Muddy Water with High Silt Content

To further investigate the vertical and horizontal pressure distribution law of muddy water with high silt content on the upstream side of the dam, a cylinder model with dimension of the 10 m in length and about 0.28 m in inner diameter is developed. The top of the model is opened while the bottom is sealed. As shown in Figure 6, the cylinder model is placed upright, with two soil pressure gauges placed horizontally and vertically at the bottom of the cylinder. The horizontal pressure gauge is used to measure the vertical pressure of muddy water, while the vertical pressure gauge is used to directly measure the horizontal pressure at the same position. A valve for discharge silt sediment is also welded at the bottom of the model to drain the muddy water and sediment.

The physical model is shown in Figure 7. The vertical pressure gauge in model is 20 cm away from the bottom, and the horizontal pressure gauge is 35 cm. The water head of vertical pressure gauge is 9.80 m.

As shown in Figure 8, the soil pressure gauge is fixed on a self-made base before placing it in the cylinder model to prevent the pressure gauge from being affected by buoyancy.

Model tests of muddy water with different silt contents are conducted, and then, the vertical and horizontal pressures of the muddy water measured by the test are analyzed and studied. The silt content of muddy water is 96.8 kg/m^3, 253.0 kg/m^3, 379.4 kg/m^3, 600.8 kg/m^3, 790.5 kg/m^3, and 1075.1 kg/m^3, respectively.

The model test steps are as follows:

(1) According to the needed silt content, the required masses of silt and water are calculated by formula (3) and weighed

(2) As shown in Figure 9, the water and silt are mixed and stirred evenly to prepare muddy water with different silt contents

(3) The prepared muddy water is injected slowly from the top of the cylinder model into a cylinder where pressure gauge is installed at the bottom (see Figure 10)

(4) After the muddy water is injected, the data of two pressure gauges are read, as shown in Figure 11. They are read again at intervals of 2–10 h until the measured data are basically unchanged

(5) The horizontal pressure P_1 and vertical pressure P_2 are calculated according to the read data and formula (4)

5. Experiment Results and Analysis

5.1. Results and Analysis of Imitation Tests. After the imitation tests, the observed muddy water is viscous and flowable, which meets the basic assumption of fluid mechanics. The calculation assumption of the vertical pressure P_2 is appropriate. And the water pressure calculation method of formula (1) can be used to calculate the pressure of muddy water with high silt content. The difference between the horizontal pressure P_1 and vertical pressure P_2 and their ratios are calculated from the calculated P_1 and P_2, respectively. The calculation results are summarized in Table 2.

According to fluid mechanics theory, the pressure of liquid is equal in all directions. Table 2 shows that the

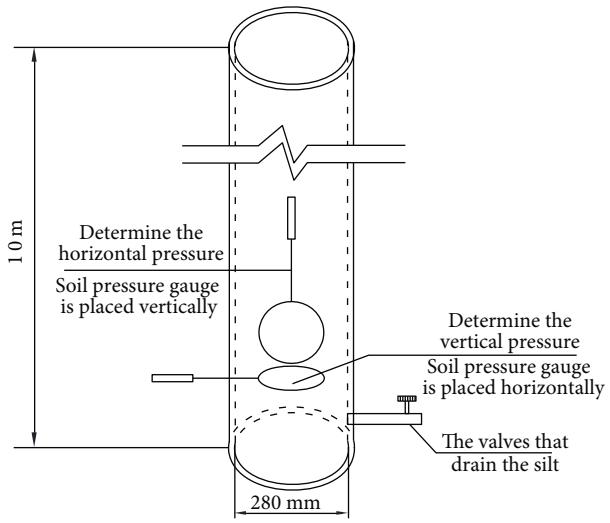

Figure 6: Diagram of the cylinder model.

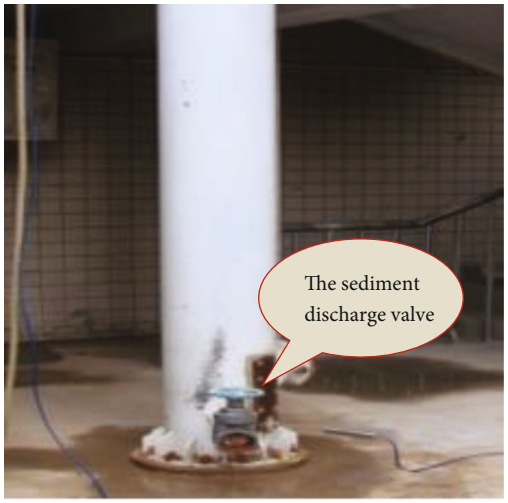

Figure 7: Physical diagram of the cylinder model.

Figure 8: The fixing of soil pressure gauge.

Figure 9: Preparation of muddy water.

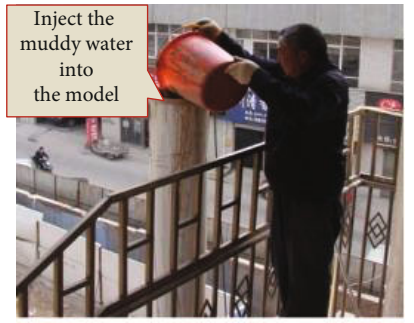

Figure 10: Inject the muddy water into the cylinder model.

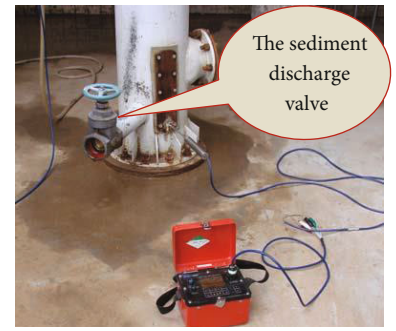

Figure 11: Read the soil pressure gauge data.

horizontal pressure P_1 is smaller than the vertical pressure P_2 in the imitation test results of each group of muddy water. The curve of P_1-P_2 and P_1/P_2 with external pressure value is plotted, as shown in Figures 12 and 13.

The curves indicate that the P_1-P_2 value fluctuates with the increase in external pressure value, but the fluctuation range is small with a maximum of 2.9 kPa, which is only 1.4%, and the P_1 values are all slightly less than the P_2 values. Analysis shows that this is due to the external pressure of the pressure tank pressured from the top of the muddy water, and some energy is lost when the pressure passes to the bottom. Thus, the measured P_1 is smaller than the calculated P_2.

Table 2: Imitation test results of each group.

Silt content	External pressure value (kPa)	The horizontal pressure P_1 (kPa)	The vertical pressure P_2 (kPa)	P_1-P_2 (kPa)	P_1/P_2
110.7 kg/m^3	50	54.3	55.4	-1.1	0.980
	100	104.3	105.4	-1.1	0.990
	150	154.8	155.4	-0.6	0.996
	200	203.6	205.4	-1.8	0.991
	250	254.1	255.4	-1.3	0.995
	300	304.9	305.4	-0.5	0.998
	350	355.3	355.4	-0.1	1.000
	400	404.8	405.4	-0.6	0.999
284.6 kg/m^3	50	54.7	55.9	-1.2	0.979
	100	103.6	105.9	-2.3	0.978
	150	154.8	155.9	-1.1	0.993
	200	203.7	205.9	-2.2	0.989
	250	253.6	255.9	-2.3	0.991
	300	303.6	305.9	-2.3	0.992
	350	353.1	355.9	-2.8	0.992
	400	403.8	405.9	-2.1	0.995
395.3 kg/m^3	50	55.9	56.3	-0.4	0.993
	100	105.2	106.3	-1.1	0.990
	150	154.2	156.3	-2.1	0.987
	200	203.4	206.3	-2.9	0.986
	250	253.5	256.3	-2.8	0.989
	300	303.4	306.3	-2.9	0.991
	350	354.1	356.3	-2.2	0.994
	400	404	406.3	-2.3	0.994
723.7 kg/m^3	50	56.8	57.3	-0.5	0.991
	100	105.7	107.3	-1.6	0.985
	150	156.8	157.3	-0.5	0.997
	200	206.4	207.3	-0.9	0.996
	250	255.1	257.3	-2.2	0.991
	300	306.6	307.3	-0.7	0.998
	350	356.7	357.3	-0.6	0.998
	400	405.7	407.3	-1.6	0.996
1059.3 kg/m^3	50	57.6	58.4	-0.8	0.986
	100	107.2	108.4	-1.2	0.989
	150	158	158.4	-0.4	0.997
	200	206.9	208.4	-1.5	0.993
	250	258.2	258.4	-0.2	0.999
	300	308.2	308.4	-0.2	0.999
	350	357.9	358.4	-0.5	0.999
	400	408.1	408.4	-0.3	0.999

The P_1/P_2 value also fluctuates slightly with the increase in imitated water head, but the fluctuation is not more than 2%. When the water head is greater than 300 kPa, the P_1/P_2 tends to be stable. The ratio is closer to 1.0 when the silt content is higher. That is, the horizontal pressure of muddy water with high silt content is equal to the vertical pressure as well.

The variation in the muddy water pressure with silt content of 1059.3 kg/m^3 over standing time is further tested in the imitation test to analyze the variation law of pressure distribution of muddy water with high silt content over time. The initiated water head is constant at 300 kPa, and the test duration is 240 h. The results are shown in Table 3.

For the water head is imitated using external equipment to pressure, it will cause a small oscillation of the muddy water in the tank, resulting in small fluctuations in the data measured by the high-precision soil pressure gauge. Therefore, Table 3 shows that, when the imitated water head is

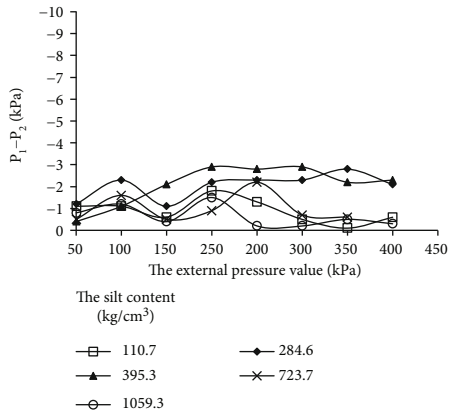

Figure 12: The curve of P_1-P_2 with external pressure.

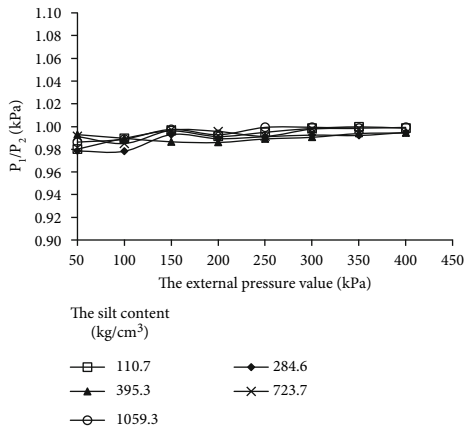

Figure 13: The curve of P_1/P_2 with external pressure.

300 kPa, the measured P_1 fluctuates with time and decreases slightly, but the variation is less than 1%. Moreover, the P_1 values are always slightly less than the P_2 values, but the P_1/P_2 values are greater than 0.99. Therefore, $P_1 = P_2$. That is, the characteristics of equal pressure in all directions of muddy water are time independent.

The comprehensive analysis of the imitation test results shows that, in the closed pressure tank, muddy water with silt content of 110.7–1059.3 kg/m^3 is viscous and flowable when the imitated pressure is 50–400 kPa, which is consistent with the basic assumption of fluid mechanics. Formula (1) can be used to calculate the pressure of muddy water with high silt content of this range. The horizontal pressure of each group muddy water is equal to the vertical pressure, and this equivalent relationship does not change with the standing time of muddy water. It is considered that the pressure of muddy water with high silt content is also equal in all directions, that is, $P_1 = P_2$.

5.2. Results and Discussion of Model Tests. The above mentioned imitation tests show that the pressure of muddy water can be measured with soil pressure gauge and calculated according to formula (1). A cylinder model is made to conduct the model test, and the pressure calculation method of muddy water with high silt content is further studied. The prepared muddy water is injected into the cylinder model, and the reading of the pressure gauge placed in the model is read until the reading is stable. The test time ranges from 50 h to 200 h.

After the test, the silt sediment of each group muddy water is collected, and its unit weight and water content are tested. The results are shown in Table 4.

The water content of the silt deposit is measured to use a density bottle method and is greater than the liquid limit of the test silt (25.9%), and the lateral pressure coefficient of silt sediment can be considered equal to 1.0 [5]. As shown in Figures 14 and 15, the change rules of horizontal P_1 and vertical pressure P_2 with test time in each group of muddy water are drawn.

From Figures 14 and 15, it can be seen that during the tests, the P_1 and P_2 of each group muddy water first decrease sharply with the test time, then slowly decreased, and finally tend to be stable. The P_1 and P_2 of muddy water with a silt content of 1075.1 kg/m^3 in group 6 are higher than those in other groups.

The analysis shows that silt particles in muddy water will settle due to self-weight, and the particles rub with the inner wall of the cylinder during the sedimentation. Meanwhile, the inner wall generates an upward force on the muddy water. Thus, the tested P_1 and P_2 all gradually decrease over time first. After the silt deposition is completed, the friction tends to be 0, and the measured pressure also reaches a relatively stable value accordingly.

Further analysis shows that the position height difference between two pressure gauges placed at the bottom of the cylinder for measuring the horizontal and vertical pressures of muddy water is 15 cm. Accordingly, the theoretical calculation value should be $P_2 > P_1$. Therefore, we correct the test data of model tests by depth according to the formula $P'_{1i} = P_{1i} + \gamma_i \times 0.15$. The relationship curves between $P_{1i}{}'/P_{2i}$ of each group of muddy water and test time are shown in Figure 16.

Figure 16 shows that the ratio $P_{1i}{}'/P_{2i}$ fluctuates slightly with test time after the correction of depth difference for P_{1i} in each group, but the magnitude does not exceed 0.5%. Therefore, we can consider that $P_{1i}{}' = P_{2i}$. The model tests prove again that the pressure distribution law of muddy water with high silt content is equal in all directions.

The pressure at a certain depth of the muddy water is calculated according to the formula of liquid pressure in the fluid mechanics theory $P = \gamma_w h$. Then, we calculate the difference between the theoretical calculated P_{1C} and P_{2C} and measured P_1 and P_2 of each group through formulas (5) to (8), respectively. The changes in ΔP_{1i} and ΔP_{2i} with test time are drawn as shown in Figures 17 and 18.

$$P_{1C} = \gamma_i \times 9.65, \tag{5}$$

$$\Delta P_{1i} = P_{1C} - P_{1i}, \tag{6}$$

$$P_{2C} = \gamma_i \times 9.8, \tag{7}$$

$$\Delta P_{2i} = P_{2C} - P_{2i}, \tag{8}$$

Table 3: Data of muddy water pressure varying with time with silt content of 1059.3 kg/m^3.

Test time (hours)	External pressure value (kPa)	The horizontal pressure P_1 (kPa)	The vertical pressure P_2 (kPa)	P_1-P_2 (kPa)	P_1/P_2
0	300	308.2	308.4	-0.2	0.999
1.4	300	307.6	308.4	-0.8	0.997
3.5	300	307.2	308.4	-1.2	0.996
7	300	307.4	308.4	-1	0.997
23	300	306.8	308.4	-1.6	0.995
29.6	300	306.7	308.4	-1.7	0.994
47.3	300	307	308.4	-1.4	0.995
72.2	300	306	308.4	-2.4	0.992
76.2	300	305.7	308.4	-2.7	0.991
144.7	300	306.4	308.4	-2	0.994
240.0	300	307.4	308.4	-1	0.997

Table 4: Basic physical parameters of silt deposit.

	Initial state of muddy water		Physical parameters of silt deposit		
Group number	Silt content (kg/m^3)	Unit weight (kN/m^3)	Unit weight (kN/m^3)	Water content (%)	Test time (hours)
1	96.8	10.39	17.84	39.1	51.5
2	253	11.34	18.62	30.7	89
3	379.4	12.12	18.23	35.1	67.7
4	600.8	13.47	18.82	30.5	95.2
5	790.5	14.62	18.82	29.9	74
6	1075.1	16.36	19.21	27.3	192

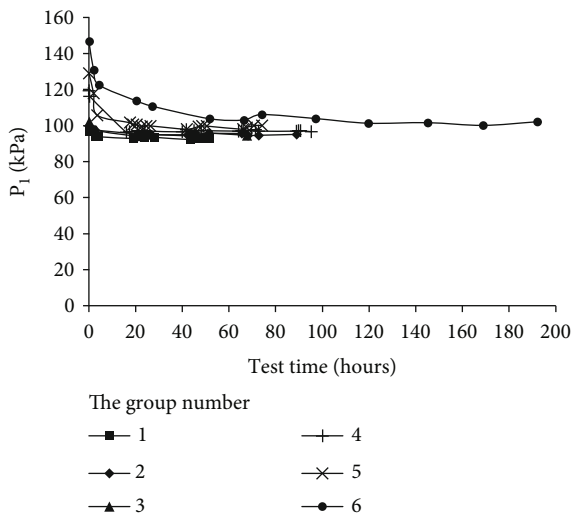

Figure 14: The change rule of P_1 with test time.

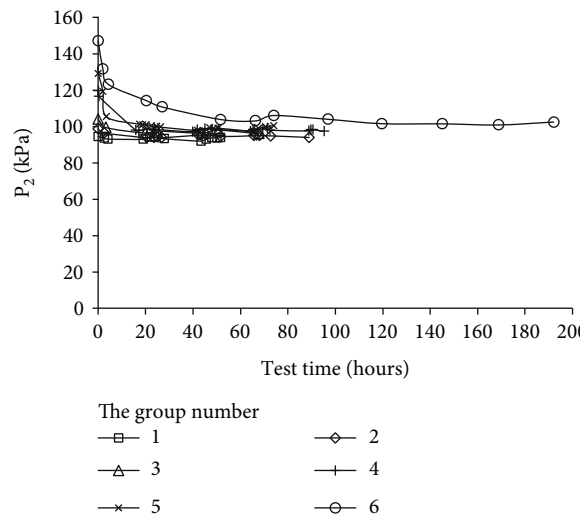

Figure 15: The change rule of P_2 with test time.

where P_{1C} and P_{2C} are theoretical calculation values of the muddy water pressure at the depth where the pressure gauge is located, γ_i is the unit weight of each group of muddy water, P_{1i} and P_{2i} are measured values of horizontal and vertical pressure, respectively, and ΔP_{1i} and ΔP_{2i} are the differences between the calculated values of horizontal pressure and vertical pressure at some moment and the theoretical calculation value.

Figures 17 and 18 show that the difference between the measured horizontal and vertical pressure values of each group and the theoretical calculation values is not equal to 0, and the ΔP_{1i} and ΔP_{2i} all increase with the rise in muddy water density. When the silt content is less than 600 kg/cm^3, the difference between the measured value of muddy water pressure and the theoretical calculation value is small. ΔP_{1i} and ΔP_{2i} greatly increase as the silt content continuously increases, and the maximum is nearly 60 kPa.

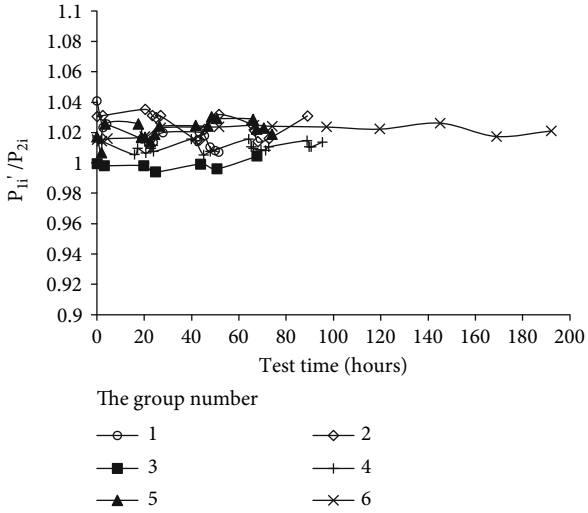

Figure 16: The relationship between P_{1i}'/P_{2i} and test time.

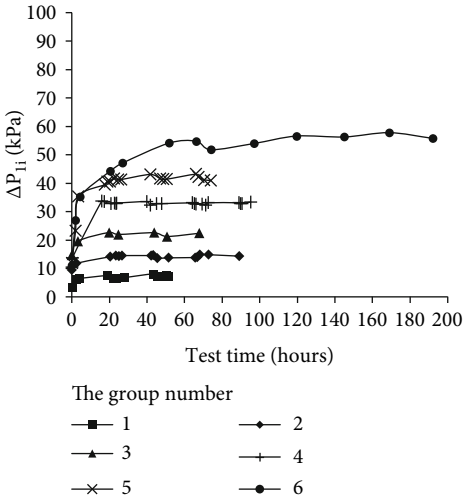

Figure 17: ΔP_{1i} change with test time.

The slope of ΔP_{1i} and ΔP_{2i} of muddy water in groups 1, 2, and 3 changes with time and is small, and the maximum value is nearly 20 kPa. However, when the silt content of muddy water is greater than 600 kg/cm^3, ΔP_{1i} and ΔP_{2i} suddenly change over time first. The change in the slope is greater when the silt content is greater, and then, it tends to be a stable value. The reason is that the silt in the muddy water has not started to settle in the early stage of the prepared muddy water poured into the model test cylinder. At this time, the unit weight of muddy water along the depth direction is equal to its design value. Then, the silt particles in the muddy water begin to settle, and the unit weight of muddy water is no longer uniform along the depth direction. Lager silt content causes faster particle precipitation and larger difference between the unit weight of the muddy water after the silt particle precipitation is stable and that at the beginning.

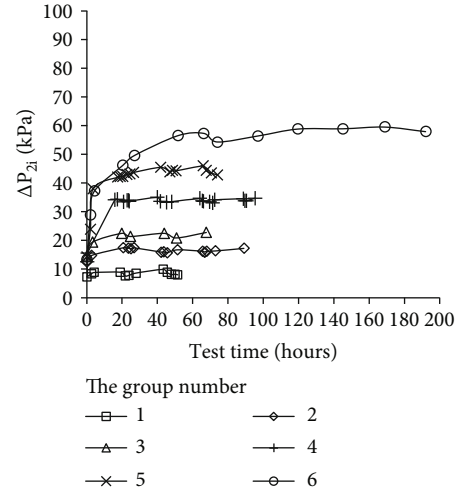

Figure 18: ΔP_{2i} change with test time.

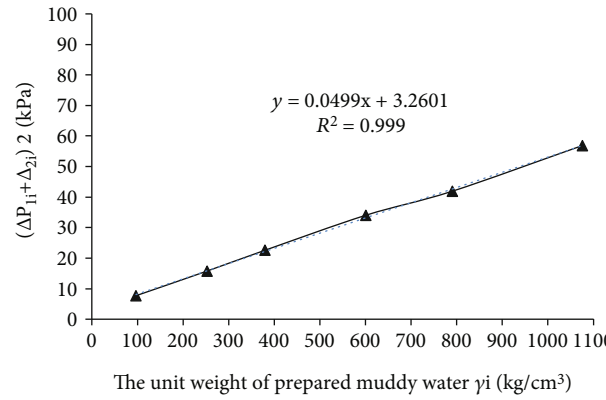

Figure 19: The relation curve between $(\Delta P_{1i} + \Delta P_{2i})/2$ and γ_i of prepared muddy water.

6. Derivation and Verification of the Pressure Calculation Formula for Muddy Water with High Silt Content

On the basis of the imitation and model tests, it can be verified that the pressure distribution law of the muddy water with high silt content is consistent with fluid mechanics theory, and the muddy water pressure can be calculated by the specification formula, that is, formula (1). However, we have no clear provision and relevant suggestions on how to determine the γ_w of muddy water with high silt content in the formula.

The horizontal and vertical pressures of the muddy water with high silt content are equal. Thus, we further analyze the ΔP_{1i} and ΔP_{2i} of each group of model test. The $(\Delta P_{1i} + \Delta P_{2i})/2$ of each group is calculated, and the relation curve with the unit weight γ_i of prepared muddy water is drawn, as shown in Figure 19.

Figure 19 shows that the $(\Delta P_{1i} + \Delta P_{2i})/2$ nearly linearly increases with the rise in unit weight of muddy water. The

Table 5: Comparison of dam stress at a water conservancy dam in China.

Silt content (kg/m^3)	Unit weight of the muddy water (kN/m^3)	Water head of the monitoring points (m)	Monitoring value of horizontal internal force (average) (kPa)	Calculation value of horizontal internal force (kPa)	Relative differences
236.5	11.24	50	547.2	558.2	1.97%
		100	1233.6	1120.2	10.12%
		150	1833.8	1688.7	8.60%

relationship between $(\Delta P_{1i} + \Delta P_{2i})/2$ and the unit weight is obtained by fitting six groups of data, as shown in

$$\frac{\Delta P_{1i} + \Delta P_{2i}}{2} = 0.0499 \times \gamma_i + 3.2601. \quad (9)$$

By combining formula (5) to (8), the actual value of muddy water pressure at a certain depth can be calculated, and the formula for calculating the pressure of muddy water with high silt content is derived as

$$P_h = \gamma_i \times (h - 0.0499) - 3.2601, \quad (10)$$

where P_h is the pressure at a certain depth of the muddy water (kPa), γ_i is the unit weight of the muddy water before the silt particle began to settle (kg/cm^3, which can be calculated by the method in the imitation tests), and h is the water head.

To verify the reliability of the derived pressure calculation formula for muddy water with high silt content, the stress of a conservancy project dam in China is calculated based on formulas (10) and (2), and it is compared with the stress monitoring value of the dam. The project is a water conservancy project with the largest storage capacity and the highest dam height in its province, including the concrete arch dam with 230 m height and water discharge, sediment drainage, and seepage prevention projects. The method used to measure dam stress is to embed the strain gauge in advance at the needed depth and calculate the corresponding stress value according to Poisson 's ratio of the strain gauge and the measured strains.

After multiple imitation calculations, the results are compared with the actual monitoring data of the project (see Table 5). The results show that, if the muddy water pressure is calculated by formula (10), then the maximum difference between the calculated and actual monitoring values is around 10%. This finding shows that the calculated value of this method is consistent with the actual monitoring value of the project, and the calculation of muddy water pressure proposed with formula (10) is reliable.

The calculation formula of muddy water pressure with high silt content derived in this study provides a strong theoretical basis and guidance for the design and calculation of dam engineering, which can avoid the waste of engineering investment. The comparison between the monitoring and calculated values also well verifies the applicability of the formula $P_h = \gamma_i \times (h - 0.0499) - 3.2601$ for calculating the pressure of muddy water with high silt content. It will provide a reliable reference and guidance for similar projects domestically and internationally.

7. Conclusions

In this study, artificial muddy water with high silt content is used to imitate the muddy water of the Yellow River with high silt content. The horizontal and vertical pressures of the muddy water are measured and calculated using high-precision soil pressure gauge, and relevant imitation and model tests are conducted. The pressure distribution law of muddy water with high silt content is tested and analyzed, and the pressure calculation formula of muddy water with high silt content is derived. The research results have certain guiding significance for similar projects and the later work of the project:

(1) In the imitation tests, the calculated value of vertical pressure of muddy water at the test depth is equal to the sum of the external pressure and the pressure calculated according to the depth of the test point. The calculated value of vertical pressure is nearly equal to the measured value of horizontal pressure

(2) The model tests verify that muddy water with high silt content is also flowable and viscous, which is consistent with the assumption of fluid mechanics theory. The fluid mechanics formula can be used to calculate the pressure of muddy water with high silt content

(3) The unit weight of muddy water can be directly substituted into formula (1) to calculate the pressure of muddy water with high silt content only before the silt particle begins to settle. However, during the process of silt particle starting to stabilize, the measured pressure and calculated values differ. The water content of the mud body settled by the silt particle of muddy water is greater than its liquid limit

(4) The pressure calculation formula of muddy water with high silt content is derived. It has been applied to a dam project. Little difference between the calculated and monitoring values is observed. These results can provide a corresponding reference and basis for the calculation of similar projects domestically and internationally

Data Availability

The data used to support the findings of this study are included within the article.

Conflicts of Interest

All the authors declare that there are no conflicts of interest regarding the publication of this article.

Acknowledgments

This study was funded by the National Natural Science Foundation of China (No. 12072260) and the State Key Laboratory of Eco-hydraulics in Northwest Arid Region of China (QNZX-2019-07).

References

[1] L. F. Yang, X. R. Wu, and F. Y. Su, "Preliminary summary of sediment problems of hydropower station in the upstream of Yellow River," *Chinese Water Power*, vol. 2, pp. 11–17, 1985.

[2] P. Hou, X. Liang, F. Gao, J. B. Dong, J. He, and Y. Xue, "Quantitative visualization and characteristics of gas flow in 3D pore-fracture system of tight rock based on lattice Boltzmann simulation," *Journal of Natural Gas Science and Engineering*, vol. 89, no. 4, p. 103867, 2021.

[3] T. Han, J. Shi, and C. Xiaoshan, "Fracturing and damage to sandstone under coupling effect of chemical corrosion and freeze-thaw cycles," *Rock Mechanics and Rock Engineering*, vol. 8, no. 5, pp. 4245–4255, 2016.

[4] J. Z. Li, *Hydraulics*, Xi'an: Shaanxi science and technology press, in Chinese, 2002.

[5] H. Tielin, W. Xianfeng, L. Dongfeng, L. Dawang, H. Ningxu, and X. Feng, "Damage and degradation mechanism for single intermittent cracked mortar specimens under a combination of chemical solutions and dry-wet cycles," *Construction and Building Materials*, vol. 213, pp. 567–581, 2019.

[6] J. X. Mai, "Quick optimal design of primary section of gravity dam," *Journal of Hydraulic Engineering*, vol. 8, no. 5, pp. 21–25, 2000.

[7] P. Hou, X. Liang, Y. Zhang, J. He, F. Gao, and J. Liu, "3D multi-scale reconstruction of fractured shale and influence of fracture morphology on shale gas flow," *Natural Resources Research*, vol. 30, no. 3, pp. 2463–2481, 2021.

[8] X. Liang, P. Hou, Y. Xue, X. J. Yang, F. Gao, and J. Liu, "A fractal perspective on fracture initiation and propagation of reservoir rocks under water and nitrogen fracturing," *Patterns and Scaling in nature and Society*, vol. 29, no. 7, 2021.

[9] T. Han, Z. Li, and Y. Chen, "Sulfate attack induced dry-wet failure modes and a constitutive model for mortar specimens with a single intermittent fracture," *International Journal of Geomechanics*, vol. 21, no. 2, p. 04020249, 2021.

[10] Z. Y. Xu, "A study of the mechanical properties of silt," *Journal of Hydraulic Engineering*, vol. 2, pp. 88-89, 1958.

[11] S. W. Chen and Z. H. Cui, "Influence of sediment pressure on the stress of gravity dam," *China Water Transport*, vol. 8, no. 5, pp. 163-164, 2008.

[12] J. Liu, Y. Xue, W. Chen, P. Hou, S. Wang, and X. Liang, "Variational phase-field model based on lower-dimensional interfacial element in FEM framework for investigating fracture behavior in layered rocks," *Engineering Fracture Mechanics*, vol. 255, article 107962, 2021.

[13] L. F. Yang, "Analysis and study of silt elevation before the dam," *Northwest Water Power*, vol. 3, pp. 1–6, 1995.

[14] T. Han and Z. Li, "Mechanical characteristics and failure modes for mode-I sandstone and rock-like cracked sample exposed to freeze thawing cycle," *Bulletin of Engineering Geology and the Environment*, vol. 80, no. 9, pp. 6937–6953, 2021.

[15] Y. M. Chen, "Effect of sediment pressure on dam under conditions of deposition and consolidation," *Engineering Journal of Wuhan University*, vol. 47, no. 2, pp. 145–176, 2014.

[16] X. Liang, P. Hou, X. J. Yang et al., "On estimating plastic zones and propagation angles for mixed mode I/II cracks considering fractal effect," *Fractals-Complex Geom. Patterns Scaling Nat. Soc*, 2021.

[17] Q. W. Han, "Distribution of dry weight of silt and its application," *Journal of Sediment Research*, vol. 2, pp. 10–16, 1997.

[18] H. Tielin, W. Xianfeng, L. Dawang, L. Dongfeng, X. Feng, and H. Ningxu, "Uniaxial deformation characteristics and mechanical model of microcapsule-based self-healing cementitious composite," *Construction and Building Materials*, vol. 273, article 121227, 2021.

[19] Z. Yin, J. Lu, and L. Wang, "Experimental study on sediment pressure before damage consolidation," *Building Information*, vol. 44, no. 19, pp. 8-9, 2017.

[20] P. Hou, S. J. Su, X. Liang et al., "Effect of liquid nitrogen freeze-thaw cycle on fracture toughness and energy release rate of saturated sandstone," *Engineering Fracture Mechanics*, vol. 258, p. 108066, 2021.

[21] T. Han, J. Shi, C. Yunsheng, and Z. Li, "Quantifying microstructural damage of sandstone after hydrochemical corrosion," *International Journal of Geomechanics*, vol. 18, no. 10, p. 04018121, 2018.

[22] S. H. Chen, *Hydraulic Structures*, China Water Power Press, Beijing, 2004.

[23] J. Liu, Y. Xue, Q. Zhang, H. Wang, and S. Wang, "Coupled thermo-hydro-mechanical modelling for geothermal doublet system with 3D fractal fracture," *Applied Thermal Engineering*, vol. 200, article 117716, 2022.

[24] T. Han, J. Shi, Y. Chen, and Z. Li, "Effect of chemical corrosion on the mechanical characteristics of parent rocks for nuclear waste storage," *Science and Technology of Nuclear Installations*, vol. 2016, Article ID 7853787, 11 pages, 2016.

[25] D. M. Duc, D. X. Thanh, D. T. Quynh, and M. Patrick, "Analysis of sediment distribution and transport for mitigation of sand deposition hazard in Tam Quan estuary, Vietnam," *Environmental Earth Sciences*, vol. 75, no. 9, 2016.

[26] D. M. Duc, M. T. Nhuan, C. V. Ngoi, T. Nghi, and D. M. Tien, "Sediment distribution and transport at the nearshore zone of the Red River delta, northern Vietnam," *Journal of Asian Earth Sciences*, vol. 29, no. 4, pp. 558–565, 2007.

[27] E. L. Eriksson and M. H. Persson, "Sediment transport and coastal evolution at Thuan An Inlet, Vietnam," *Division of Water Resources Engineering Department of Building and Environmental Technology Lund University*, vol. 29, no. 4, 2014.

[28] S. R. Chalov, J. Jarsjö, N. S. Kasimov, and A. Roomanchenko, "Spatio-temporal variation of sediment transport in the Selenga River basin, Mongolia and Russia," *Environmental Earth Sciences*, vol. 73, no. 2, pp. 663–680, 2015.

[29] Y. H. Chang, M. D. Scrimshaw, and J. N. Lester, "A revised grain-size trend analysis program to define net sediment transport pathways," *Computers & Geosciences*, vol. 27, no. 1, pp. 109–114, 2001.

[30] T. Han, J. Shi, Y. Chen, and X. Cao, "Physical and mechanical properties of marble under the combined effects of chemical solutions and freeze-thaw cycles," *Geotechnical Testing Journal*, vol. 40, no. 6, pp. 1057–1070, 2017.

[31] S. Gao and M. Collins, "Net sediment transport patterns inferred from grain-size trends, based upon definition of "transport vectors"–comment," *Sedimentary Geology*, vol. 90, no. 1-2, pp. 153–156, 1994.

[32] S. Gao and M. Collins, "Analysis of grain size trends, for defining sediment transport pathways in marine environments," *Journal of Coastal Research*, vol. 10, no. 1, pp. 70–78, 1994.

[33] X. He, Y. P. Wang, Q. G. Zhu, Y. Zhang, and D. Zhang, "Simulation of sedimentary dynamics in a small-scale estuary: the role of human activities," *Environmental Earth Sciences*, vol. 74, no. 1, pp. 869–878, 2015.

[34] A. Campisano, E. Creaco, and C. Modica, "Numerical modelling of sediment bed aggradation in open rectangular drainage channels," *Urban Water Journal*, vol. 10, no. 6, pp. 365–376, 2013.

[35] D. Mateusz, Z. Agata, and Z. Marek, "Sedimentation from suspension and sediment accumulation rate in the River Vistula prodelta, Gulf of Gdańsk (Baltic Sea)," *Oceanologia*, vol. 55, no. 4, pp. 937–950, 2013.

[36] S. Angelika and Z. Tamara, "Sediment deposition and accumulation rates determined by sediment trap and ^{210}Pb isotope methods in the Outer Puck Bay (Baltic Sea)," *Oceanologia*, vol. 56, no. 1, pp. 85–106, 2014.

[37] Z. Zuo, D. Eisma, R. Gieles, and J. Beks, "Accumulation rates and sediment deposition in the northwestern Mediterranean," *Deep Sea Research Part II: Topical Studies in Oceanography*, vol. 44, no. 3-4, pp. 597–609, 1997.

[38] The Ministry of Water Resources of the People's Republic of China, *Design Specification for Concrete Arch Dams*, China Water Power Press, Beijing, 2003.